B4W: A Smart Wireless Intruder Detection System

Sharma, Suryansh; Venkata T., Prabhakar ; Singhal, Shalakha ; Kuma, Gogineni Gopi Sunanth; Venkatesha Prasad, R.

DOI
10.1109/ICC45041.2023.10279723

Publication date
2023

Document Version
Final published version

Published in
Proceedings of the ICC 2023 - IEEE International Conference on Communication

B4W: A Smart Wireless Intruder Detection System

*Suryansh Sharma, +Prabhakar Venkata T., +Shalakha Singhal, +Gogineni Gopi Sunanth Kumar, *R. Venkatesha Prasad
*Delft University of Technology, The Netherlands, +Indian Institute of Science, India

***Abstract*—Surveillance and monitoring are highly critical in many application scenarios like wildlife conservation, restricted areas such as nuclear spillover, and border security. Moreover, in these scenarios, intrusions do not happen frequently thus, conventional surveillance is overkill and expensive that also requires extensive human involvement which can be arduous, expensive, and inefficient. To address these issues we propose an end-to-end smart acoustic surveillance solution for intrusion detection using a simple low-cost system called *Balls for Walls* (B*4*W). The objective is to create a network of sensors that could also be remotely launched. The nodes responsible for surveillance employ audio sensors which are packaged within hard balls thus allowing the launch of these sensors from a distance of over 500 m. We use microphones for detecting human activity inferred through sensing the sound of footsteps against background noise. We evaluate the systems across five different terrain types. We propose a novel, low complexity detection algorithm called SEED which leverages signal energy and shape to distinguish humans from ambient noise. B*4*W offers a maximum detection rate of 98.3% on dry leaves and a low false alarm rate of 0.9%. The system is energy efficient to last a maximum of 170 days and it is orientation agnostic. The proposed system has been extensively tested across varying terrains and ambient signal scenarios to demonstrate its efficacy.**

***Index Terms*—Wireless Sensor Networks, Localization, Surveillance, Intruder Detection, Acoustic Sensors, Edge Computing**

I. Introduction

Chernobyl and surrounding areas till date have restricted human access in large, dangerous, radioactive hot-spots caused by a major nuclear disaster of unprecedented scale. The original 30 km radius exclusion zone has been modified and now covers an extensive 4300 sq. km [1]. Numerous species from elephants to rhinos are under constant attack from poachers. The nomadic nature of these herds of animals combined with the vast open nature of wildlife sanctuaries necessitates a more innovative solution to alert authorities upon possible poacher [2], [3]. Further, the porous nature of international borders often creates disputes because of human or drug trafficking. These scenarios demonstrate a critical need for a system for detecting human presence in harsh or restricted areas to either safeguard humans themselves or animals from them. As an alternative to traditional walls or fencing, we propose a completely smart system in order to *sense-detect-communicate* based on small sensor nodes which fence an area virtually. However, in order to do this, there is an inherent set of challenges that need to be addressed. These systems rely on *planned* pre-deployed sensor nodes and the system may involve placing wearable devices on targets [4]. This is difficult to achieve when physically going to the restricted areas (like a nuclear-spill zone) is not possible and the sensors must only be deployed from a distance and possibly self-organize to form a barrier. Further, any system relying on the use of radar or cameras for sensing necessitates planned manual deployment and lacks reconfigurability which makes the sensor network static and prohibits ad-hoc deployment [5], [6]. These sensor networks require additional maintenance and consume significant power [2], [7]. Lastly, solutions based on drones, static surveillance sensor towers, and mobile nodes draw the attention of the intruders [8], [9] and may suffer from short operational times. Even satellite camera-based methods may not always work in areas requiring constant vigilance especially if the intruder is camouflaged or when there is low visibility [10]. These challenges raise an important question about the design of **a wireless sensor system for virtual sensing of restricted areas that is remotely deployable, low-power, and requires zero maintenance.**

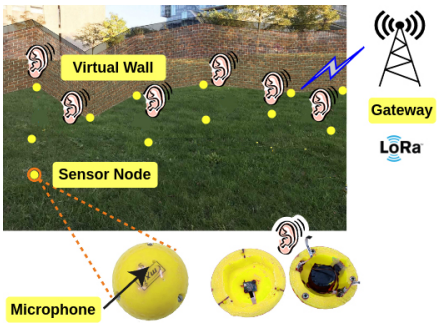

Fig. 1: Conceptual overview of B*4*W system: balls with acoustic sensors are launched and localized to form a virtual fence; will be camouflaged in actual deployment.

To overcome the above challenges, we present a comprehensive end-to-end solution called **Balls for Walls (B*4*W)** that aims to solve the problem of intruder detection. Our proposed system employs miniaturized, low power sensor nodes that are packaged into small camouflaging (golf-sized) balls that can be remotely deployed across the surveillance area. These balls form a virtual digital fence as shown in Fig. 1. The system incorporates a novel localization algorithm, combining image processing and accelerometer data to estimate the launch angles and the time of flight, thus, effectively determining the final resting position of the balls post-deployment. Three acoustic sensors (microphones oriented 120° apart) housed inside each ball are activated after deployment and using our novel detection algorithm send wireless alerts to a gateway.

Features and Contributions. ❶ We present a complete system that leverages miniaturized, low cost, low power design

ICC 2023 - IEEE International Conference on Communications | 978-1-5386-7462-8/23/$31.00 ©2023 IEEE | DOI: 10.1109/ICC45041.2023.10279723

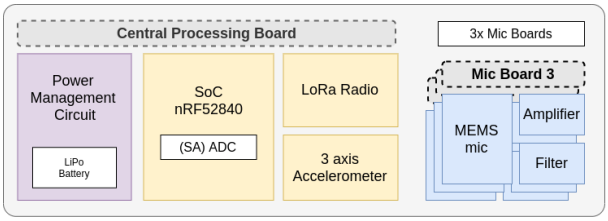

Fig. 2: Block diagram of acoustic sensor in ball.

(a) (b)

Fig. 3: Orientation of the sensor node with (a) 1 mic above mid-plane (worst case) and (b) 3 mics in mid plane (best case).

consisting of three microphones to detect human presence. To the best of our knowledge, B*4*W is the first WSN system to present an end-to-end solution for stealthy intruder detection using easily camouflaged acoustic sensors. B*4*W has all the modules embedded enabling it to act as a virtual fence (Sec. II). ❷ We provide a simple but efficient methodology for remote deployment and localization of the sensors. We avoid using GPS because of the cost, size, and power requirements, and for deployment in a possible GPS denied environments. We further demonstrate the capability of locating the sensors when deployed remotely (Sec. IV). ❸ A new low-complexity intruder detection algorithm, SEED, is developed for human intrusion detection on our specially designed low-power sensor balls which are orientation agnostic (Sec. III). We also optimize the energy usage so that the lifetime of each ball can last up to 6 months (Sec. II). ❹ We present a thorough evaluation of multiple sources of noise and collect real-world data. We deployed five balls and tested the B*4*W system thoroughly including the detection and wireless capabilities of B*4*W when the balls are subject to different terrain depending on deployment (Sec. V).

II. Sensor System Design

Acoustic detection. The choice of using acoustic sensors in the system design is motivated by several factors. Compared to other sensors like cameras, radar, or PIR motion sensors, microphones are relatively orientation agnostic and consume low power. Additionally, microphones can function when packaged inside a ball which in turn is needed for the launch and remote deployment strategy. The cost of using acoustic sensors is lower than other image-based modalities. An important system consideration is that it must be possible to keep most of the electronics in sleep mode when there are no detected intruders present. The sensing and detection modules are thus triggered only when the average is above a certain threshold.

Orientation-agnostic sensing. The sensor node is designed to have three microphones placed 120° apart as a conscious design choice given the spherical nature of the node. The

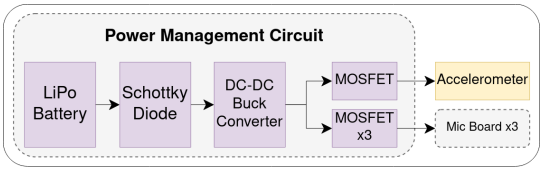

Fig. 4: Block diagram of the power management unit.

design philosophy is to make the sensor node orientation agnostic implying that irrespective of the ball orientation after landing, at least one out of the three microphones would be facing the air and not the ground. The availability of three microphones is also leveraged by the classification algorithm to strengthen its detection accuracy by combining the different inputs provided by the three microphone channels.

Central processing board. The central processing board houses an SoC - nRF52840 based on ARM Cortex M4 microcontroller with integrated Bluetooth Low Energy (BLE) radio, a 3-axis accelerometer, and a LoRa modem. The accelerometer chosen was H3LIS100DL because of its high sensitivity and low power functionality. The three microphone boards are interfaced to the central processing board's ADC channels via flexible FPC cables to enable easy positioning within the sensor node ball. As seen in Fig. 4, the power management unit contains a DC-DC buck converter LTC3246, a Schottky diode, and four MOSFETs which act as switches to independently power and control any of the three microphone boards or the accelerometer. This design allows control over the power consumption of the device by cutting power to different mic boards or peripherals based on requirement resulting in reduced power wastage. After detecting an intruder, it transmits an alert message to a remote base station using the low power long-range LoRa modem.

Microphone sensor boards. Each microphone board consists of a MEMS microphone sensor as well as a filter-amplifier block. We perform hardware filtering and amplification reducing the processing required by the microcontroller. We choose ICS-40618, a MEMS-based microphone with a differential non-inverting analog output. It has -38 dBV sensitivity (differential) and an extended frequency response from 50 Hz to 20 kHz which can detect all relevant intrusion sources. The design of the gain stage (and by extension, the microphone) board depends on the fundamental frequency ranges of different audio sources present in a real-world setting. These frequencies would be key in determining the desired bandwidth of the gain stage. To investigate this, multiple audio samples were recorded both for ambient noise as well as human intrusion scenarios with activities like talking, walking, etc. The audio for human footsteps, identified as a key factor for human presence, was further collected for different terrains. The key insight was that different terrains and topographies will result in different audio signatures. We derived the Fast Fourier Transform (FFT) of the recorded time series audio sequences. Fig. 5 shows the frequency range chart for the different sounds considered. This formed the basis for the design of the filter and amplifier blocks as well as for the

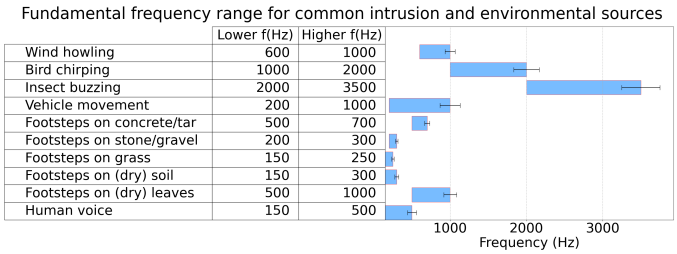

Fig. 5: Measured **f**(Hz) ranges for common intrusion sources

TABLE I: Measured Channel Activity Detection(CAD) success (for one symbol duration) with varying Spreading Factors(SF) for 5 m separation between nodes

LoRa SF	SF7	SF8	SF9	SF10	SF11	SF12
CAD success	100%	100%	97.2%	92.5%	100%	100%

audio detection algorithm. From Fig. 5 it can be noted that the frequency of interest lies between 200 Hz to 1 kHz. Hence, the -3 dB bandwidth of the gain stage was designed to be greater than 10 kHz. Therefore, we also set the sampling rate of ADC channels to 10 kHz. The gain stage required to have high input impedance, high gain, high -3 dB bandwidth, and low current consumption. Op-Amp MIC862 was chosen as the amplifier due to its low supply current of only 31 μA and gain bandwidth of 3 MHz. A DC blocking capacitor is used to isolate the gain stage from the DC offset of the microphone output.

LoRa for communication. LoRa is employed to establish a long-distance link from each node to the base station (located at a faraway distance). The central board has an RFM95W LoRa modem which allows a maximum link budget of 164 dB and the module can be controlled via SPI interface. Two important parameters that must be configured are spreading factors and the bandwidth. The only requirement that the system imposes is to select different values for these two parameters for adjacent nodes in the network during deployment. Selecting a single frequency can lead to interference issues if many neighboring nodes detect an intruder. We use the Channel Activity Detection (CAD) mechanism of LoRa to prevent potential collisions when simultaneous packet transmissions occur at adjacent nodes after intruder detection. Standard CAD in LoRa is usually implemented with 4 symbol time but we use one symbol to reduce waiting time and can therefore transmit faster with a smaller contention window. If two nearby nodes want to simultaneously transmit, one of them will get delayed due to CAD thereby avoiding an imminent collision. Table I shows the percentage of successful CAD measured with our scheme of one symbol duration. The higher success rate of CAD for our scenario is because two nodes that detect the same intruder must be physically close to each other. Therefore, RF power would be high leading to a higher percentage of detection even if a single symbol CAD is executed. After detecting an intruder, each node waits for a random period between [0 10] symbol times before sending a LoRa frame to reduce the collision probability. After this random time, it executes CAD for one symbol period. If it finds that there is an ongoing transmission, it waits till

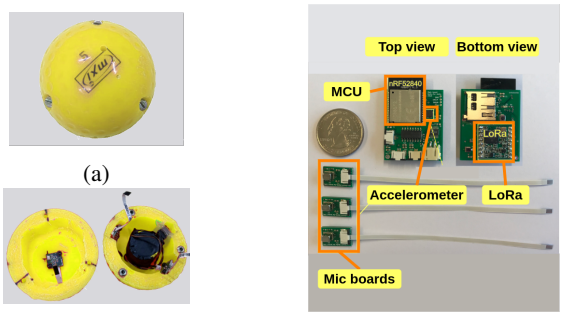

Fig. 6: (a) Packed (b) Open (c) Components of B*4*W node.

TABLE II: Measured current consumption of the various modules and estimated lifetime for different scenarios

System State	**Current**
System startup	19.25 mA
Ball Launched	5.5 mA
Sleep; accelerometer disabled; waiting for intrusion	0.4 mA
Intrusion detection and processing	2.4 mA
LoRa Transmission(event based)	8-10 mA
Deployment Scenario	**System lifetime**
Single mic board enabled at a time	170 days
Only 2 mic boards enabled simultaneously	135 days
All 3 mic boards enabled all the time	102 days

the completion of the current transmission, thereby avoiding potential collisions. The node that sends later due to waiting also includes the total time it waited after detection within the LoRa frame so that the gateway can identify that the same intruder was captured by more than one node at the same time showing high temporal correlation and indicating higher confidence in the detected event.

Design of the enclosure. The remote launching and deployment of the sensor nodes in inaccessible regions require an innovative approach in enclosure design. This is to ensure proper sensing and functionality after landing. The application necessitates a novel packaging solution that is small in size, can sustain impact during deployment, and safeguard the embedded hardware from environmental damage. It must also not impede radio performance while still providing air exposure to the microphone inputs. Considering the component dimensions and packaging requirements, a ball with a diameter of 70 mm with a symmetrical arrangement of depressions on its surface was selected for packaging. The dimpled balls when moving through air experience more lift and less drag thus, flying farther than smooth balls. Figure 6(c) shows the sensor node with its components. The central processing board is connected to the three microphone boards using three FPC cables, each being 120° apart to provide 360° coverage for a single node as seen in Fig. 6(b). Three holes on the periphery of the ball provide air exposure for the microphones. The sensor boards are fixed inside the ball using screws to avoid displacement. Figure 6(a) shows a packaged sensor node with the two hemispheres arrested together.

Energy Optimization. The sensor nodes are powered by a 3.7 V 2000 mAh battery and are deployed remotely in inaccessible terrains. There is, therefore, a need to maximize

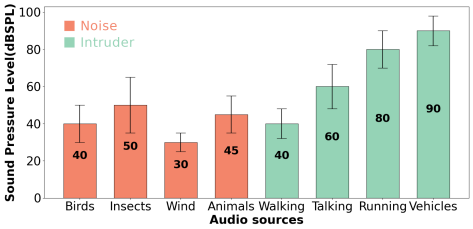

Fig. 7: Acoustic pressure levels for different audio sources

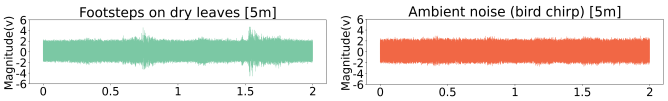

(a) (b)

Fig. 8: Signal comparison between (a) intruder walking on the dry leaves and (b) bird chirping, at 5 m.

their lifetime to keep the virtual fence active and without gaps. The system employs an onboard comparator before the audio signal is fed to the MCU for sampling. The role of the comparator is to check the analog signal value and generate an interrupt to wake up the MCU only if the signal amplitude exceeds a predefined threshold which is set above the noise floor ensuring that the MCU is not powered unless the actual computing necessitates it. This results in power saving. Table II shows the measured current consumption of each component in the node. We calculate that the CPU and ADC are running for 400 ms after an event is detected by the comparator and assume the frequency of intrusion to be limited to one per day. When no intrusion occurs, the MCU is in sleep mode. The average current consumption is 0.45 mA(1 mic enabled at a time). When an intrusion occurs, the CPU and ADC are running. The total current consumption is 2.4 mA (1 mic enabled at a time). Using these measurements, the lifetime is estimated to be 170 days. The system lifetime will reduce to 102 days in the worst-case scenario when all three microphones are enabled.

III. Detection Algorithm

Signal energy detection. The system uses signal amplitude as a critical metric to detect signs of intrusion. To characterize potential high amplitude ambient noise that the sensor nodes may encounter (ex: birds, insects, animals, wind) the sound pressure level of various sources of interest was captured(Fig. 7). The noise sources were all located more than 5 m while the human sources were located at 5 m from the nodes. The energy detected in the captured signal is used as a feature by the classification algorithm.

Signal Shape Characterization. Signal energy detection, however, will only work when the ambient noise sources are located much farther away than the intruders, i.e., SNR is high. Therefore, there is a need to use spectral features of the signal for preventing large false positives when animals or birds come near the balls. Fig. 8 shows an example of the shape of two captured audio signals belonging to the two classes [intruder, noise]: an intruder walking on dry leaves (forest floor) in the presence of ambient jungle noise and a bird chirping. Both of the sources are located at 5 m from the node. It shows signal shape to be useful for differentiating noise and intruder audio. We are inspired by a speech classification algorithm-Time Encoded Signal Processing and Recognition(TESPAR) that leverages zero-crossings points of the audio signal to achieve mean random-word intelligibility score of 97.9% [11].

Shape Encoded Energy Detection(SEED). We propose a simple yet novel algorithm for our nodes which combines energy information (amplitude) and the spectral information (size of zero crossing intervals) of the audio signal. This low complexity algorithm ensures a high intrusion detection accuracy and with reduced false detection. The audio signal is divided into epochs of 2 s intervals and fed as input to the algorithm. The node checks the orientation of the ball and selects mic channel m to sample based on the number of mics above the midplane to obtain signal V_m. The sum of the values of the positive (or negative) peaks of the signals is used to get a voltage value called V_p. This value signifies the energy contained in the signal. Next, it is compared to a reference threshold V_{th} to see if the signal contains a possible event. V_{th} is based on the environment where the system is deployed and is influenced by the noise floor in that region. The input signal is hardware filtered and DC offset removed. Hence, the sum of positive peaks (not DC offset) is calculated. If the resultant does not exceed the preset threshold then the system classifies it as noise. However, if V_p does exceed the V_{th} value then the signal is further processed to ensure that a real event is not dropped. We count the samples between two successive zero crossings in an epoch array D. The D values effectively represent the widths of different epochs present between any two successive zero crossings. Then we find the distribution of D values. The frequency of occurrence of D values is calculated for the entire input signal and stored in an Z array. The successful distinction of human intruders from ambient noise depends on the on the Z array values. We create a training database by collecting multiple audio samples and constructing signal archetypes for both audio classes (human intruder and ambient noise). These signal archetypes are created by averaging the Z arrays of different signals from the same audio source. Once Z is found, it is compared with the archetypes stored in the training database using the K-nearest neighbour (KNN) machine learning technique, which uses the Manhattan distance between Z arrays to classify the signal. The prediction is chosen as the class with the least distance to the test signal. This process is carried out by the sensor node for each mic m that is considered active. The final classification decision is made after the majority voting between the different mic channels in the node. The training database is used to set the noise threshold value V_{th} in the sensor node based on the noise.

IV. Remote Deployment and Localization

We propose a novel approach to remotely deploy these sensor nodes using a launcher and subsequently perform localization to create a virtual barrier. Our localization algorithm is agnostic to the launch mechanism used. It is essential to

Algorithm 1: SEED algorithm for intrusion detection

Result: Prediction value where 0 is no detection and 1 is intrusion

Prediction = -1;
Check orientation of sensor node to select mic channel m where m = [1,3] and obtain V_m;
Obtain $V_p = \sum$ i for i > 0 in V_m;
if $V_p > V_{th}$ **then**
  Calculate Z array = [frequency for each zero crossing D value];
  Calculate Manhattan Distance d_n (noise) and d_h (human) of Z for all training archetype ;
  Apply KNN algorithm to select archetype from each class with the least distance;
  if $d_1 < d_0$ **then**
    Set $Prediction_m$ = 1; Human detected by mic;
  else
    Set $Prediction_m$ = 0; Noise detected by mic;
else
  Set $Prediction_m$ = 0; Noise detected by mic;
Repeat to obtain $Prediction_m \forall$ selected m;
if *Majority* $Prediction_m$ = *1* **then**
  Prediction = 1;
else
  Prediction = 0;

Algorithm 2: Proposed image processing algorithm for angle of launch and heading

Result: Launch angle, Heading angle

Extract frames from each 240 fps video;
Create HSV color mask for color thresholding of frame based on ball color;
Subtract background by element wise (pixel wise) subtraction of consecutive color threshold frames;
if $Value_{pixel}$*=0* **then**
  Signify stationery objects of frame (suppressed);
else
  Signify movement between consecutive frames;
Apply Hough circle transform to detect circles in frame;
if *Circle detected in frame* **then**
  Store Centre(x,y) and Radius(r) of detected circle;
else
  Discard frame;
if *Centre(x,y) lies in Region of Interest(RoI)* **then**
  Ball present in expected (pre-defined) region of interest, calculate angle;
else
  Detected circle is outlier, discard the frame;
Plot centre(x,y) of circles from 8 frames and find best fit linear regression;
Calculate angle from slope of obtained line;

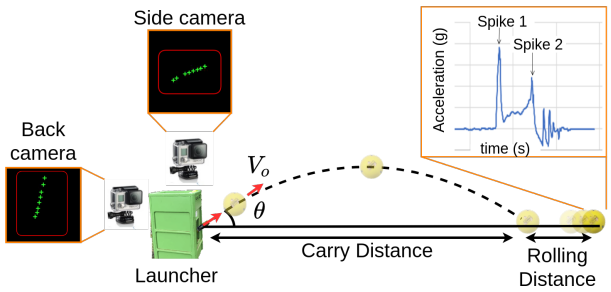

Fig. 9: Projectile: launch trajectory and localization

estimate the deployed node's final resting position in a no-network zone for successful localization.

Estimation of first landing location. Any object that is thrown or launched moves along a curved path under the gravitational pull and the physics of this projectile motion is exploited by our algorithm. The horizontal component of velocity of the ball is constant and is given by, $v_x = v_o \cos\theta$ where, v_o is the launch velocity and θ is the launch angle. The equations for time of flight (t) and carry distance x are: t = $\frac{2v_o \sin\theta}{g}$ and x = $\frac{v_o^2 \sin 2\theta}{g}$, respectively. The first landing location of the ball can thus, be estimated if the parameters, initial velocity, launch angle and time of flight are known. If a ball cannon is used for launching it is possible to configure the initial velocity of the ball while the angle of the launch can be controlled by changing the angle of the cannon. However, if the balls are launched manually then it is important to measure these basic quantities with reliable accuracy. We calculate the carry distance (distance between first landing and launch location) by finding the launch angle and time of flight. Further, we estimate the heading direction angle in which the ball was launched. Two orthogonal high frame-rate cameras, GoPro Hero 3, are used to capture the initial trajectory of the launched balls accurately. The side camera is used to calculate the launch angle while the back camera is used to calculate the angle of heading. We propose a novel image processing (algorithm 2) to this end. The Region-of-Interest based thresholding step makes the algorithm robust, devoid of any outliers, and also avoids fish-eye distortion. Fig. 9 shows the plots of detected center points for both cameras. We observe that eight detected center points (eight frames) are sufficient to accurately calculate the angles. The accelerometer embedded inside the sensor node is used to determine the time of flight. The acceleration values in X, Y, and Z are read every 20 ms and their quadratic mean is calculated. Figure 9 shows the accelerometer data received after the launch of a sensor node. From this, we can calculate the time of flight using T = (Spike 2 packet no. - Spike 1 packet no.) $\times$ 20 ms.

Estimation of final resting location. We observe that the acceleration value becomes constant after the ball comes to rest (at 8.5 s) in Fig. 9. Therefore, we can calculate the rolling / bouncing time duration after its first contact with the ground. Rolling time calibration is done to estimate the rolling distance of the ball with reasonable accuracy. From the first landing location and rolling distance we can estimate the final resting

(a) Dry leaves terrain (b) Grass terrain (c) Stone terrain (d) Concrete terrain (e) Soil terrain

Fig. 10: Experimental setup for testing intrusion detection across varying terrain

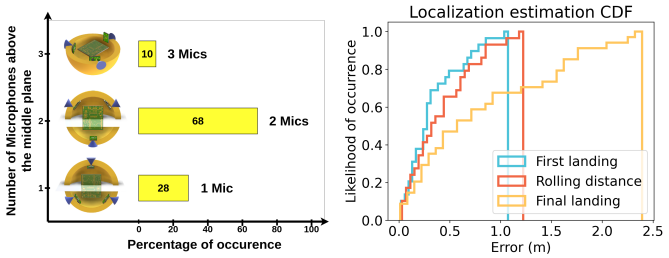

(a) (b)

Fig. 11: (a) Distribution of ball orientation after deployment; (b) CDF of the localization estimation results

location of the nodes. If the landing terrain data is available along with the rolling time, the location estimation can further incorporate this information for even non-uniform terrain. This makes the algorithm robust and enables the remote deployment of our sensor nodes even from a large distance.

V. Experiment Setup and Evaluation

Data were collected from four different ambient noise sources: wind, insects, bird chirps, and animal motion (cows, dogs, and cats) and of audio which signalled human presence: a person talking, running, jogging, and walking. Further, data was also collected for varying numbers of people walking (intruders could only be walking/running to cross the virtual fence). We also varied the distance of the human source from the sensor between 1 m to 5 m. Lastly, audio data was also collected for a person walking on different terrains shown in Fig. 10. A total of 1000 2 second recordings were collected for both audio classes. All of the audio of the second class was randomly interleaved with the noise audio samples to result in various background noises sources being intermixed to simulate real life scenarios. A tennis ball cannon is used to set the launch angle of the balls and other parameters like the elevation angle and launch speed are controlled. The localization experiments are carried out in an open field with low elevation. 5 sensor balls are launched 20 times to 500 m and the orientation and location data are collected each time. The LoRa transmission characteristics of nodes when they are covered by various terrain and on surface are studied. The impact of the capture effect resulting from the simultaneous transmission of two nodes is also analyzed.

Deployment: Ball orientation. We evaluated the distribution of node orientation after deployment. Five nodes were launched 20 times to obtain the distribution as shown in Fig. 11(a). It can be observed that 68% of the times at least 2 microphones were above (or in) the middle plane after launching providing an opportunity to use signals from one of the two channels, increasing the detection probability.

TABLE III: Comparison of SEED with Energy detection (ED) and standard TESPAR (T) for all terrains and noise sources.

SEED	I	N
I	93.3	6.7
N	6.9	93.1

ED	I	N
I	92.3	7.7
N	38.2	61.8

T	I	N
I	90.1	9.9
N	46.8	53.2

Deployment: Localization accuracy. The cumulative distribution of localization accuracy after deployment is shown in Fig. 11(b). We observe that the final resting location of the ball is estimated within a reasonable accuracy of 2.4 m even in the worst case and within 1 m for 70% of the cases.

Intruder detection: The performance metrics considered are Detection rate (DR) = $\frac{TP}{TP+FN}$, False Alarm Rate (FAR) = $\frac{FP}{TN+FP}$. The DR, FAR, and confusion matrix are obtained after performing 10-fold cross-validation on the data-set. **(I) Intruder activity.** The performance of the detection algorithm is tested for different intrusion activities (talking, running, jogging, or walking). Fig.12(a) shows the performance metrics when one person performs these activities at a distance of 1 m. **(II) Number of people.** The next intrusion scenario considered a different number of people walking next to the sensor node. Fig.12(b) shows the results with 1 to 5 people. **(III) Terrain type.** We evaluated the performance for five different terrains shown in Fig. 12(c). We observe that for all five scenarios the DR is 85% or above. The FAR is also always below 10%. **(IV) Distance from node.** We evaluated the accuracy of the system when the intruder is at varying distances from the node. This result is presented in Fig. 13. **(V) Comparison.** Table III shows the confusion matrix for SEED compared to energy detection and TESPAR. SEED outperforms the others in terms of both DR and FAR. TERPAR has high FAR due to the encoding of signals without energy consideration. SEED solves this issue (low FAR) while maintaining low complexity.

LoRa: (I) Link with varying terrain. The LoRa RSSI values were evaluated for different terrains completely occluding the nodes. The gateway was located at a distance of 250 m from the nodes. Fig. 14 shows that a sufficient communication link could be maintained for all scenarios. **(II) Capture effect.** The LoRa paradigm developed to prevent frame collisions when multiple balls transmit using CAD and capture effect(Sec.II) was evaluated. Fig. 15 shows the results of this experiment for two adjacent nodes and are congruent with those expected in [12]. With power difference and delay (when CAD fails) we see that at least one of the transmissions reaches the gateway. These results provide the confidence in B*4*W using LoRa with

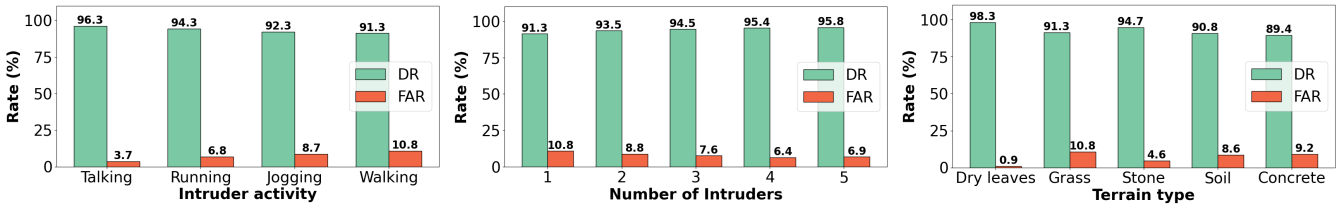

(a) (b) (c)

Fig. 12: Intruder detection performance with varying (a) intruder activity, (b) number of intruders and (c) terrains.

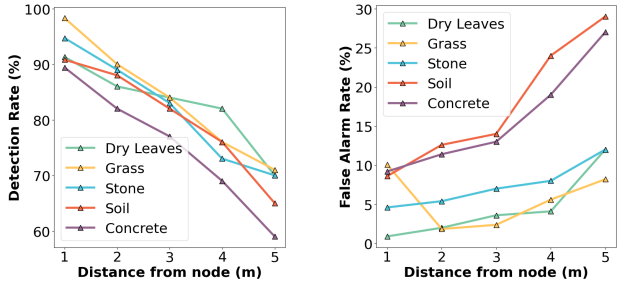

(a) (b)

Fig. 13: (a) DR and (b) FAR with varying distance and terrain

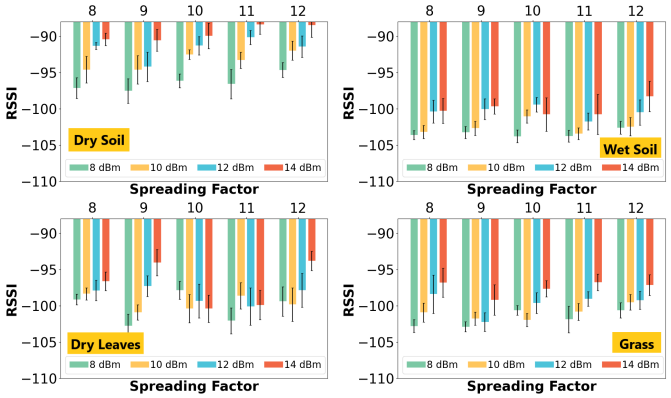

Fig. 14: LoRa characteristics with varying transmit power and SFs for nodes under different terrain occluding them

minimal required coordination amongst the nodes.

VI. Conclusion

We developed an intruder detection system called *Balls for Walls* (B*4*W) to address many use-cases such as securing wildlife from poachers, finding inadvertent entry into dangerous areas and border security. We designed a miniaturized acoustic sensing system embedded inside rigid balls. We proposed a novel, low complexity algorithm called SEED and optimized the system for a long lifetime. We presented a remote deployment algorithm which utilized image processing and accelerometer data to accurately localize our spherical nodes with a worst-case error of 2.4 m. We characterized the LoRa link showing that reception is possible even with two transmissions colliding and built a CAD based mechanism to avoid collisions. We performed a thorough evaluation of intruder detection with SEED to achieve a low false alarm rate (≈10%) and with a maximum detection rate of 98.3% also evaluating different intrusion scenarios across five different terrains. We also studied the effect of various terrain obstructions on the transmission characteristics of nodes.

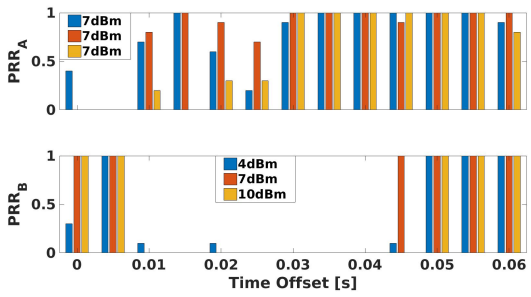

Fig. 15: PRR for simultaneous LoRa transmissions by 2 adjacent nodes 3 m apart with varying time delay of transmission

References

[1] "Chernobyl accident 1986," Apr 2020. [Online]. Available: https://www.world-nuclear.org/information-library/safety-and-security/safety-of-plants/chernobyl-accident.aspx

[2] J. Kamminga, E. Ayele, N. Meratnia, and P. Havinga, "Poaching detection technologies—a survey," *Sensors*, vol. 18, no. 5, p. 1474, 2018.

[3] E. R. Buhuş, L. Grama, and C. Rusu, "Several classifiers for intruder detection applications," in *2017 International Conference on Speech Technology and Human-Computer Dialogue (SpeD)*, July 2017.

[4] D. M. Anderson, "Virtual fencing–past, present and future1," *The Rangeland Journal*, vol. 29, no. 1, pp. 65–78, 2007.

[5] A. Arora, P. Dutta, S. Bapat, V. Kulathumani, H. Zhang, V. Naik, V. Mittal, H. Cao, M. Demirbas, M. Gouda, Y. Choi, T. Herman, S. Kulkarni, U. Arumugam, M. Nesterenko, A. Vora, and M. Miyashita, "A line in the sand: A wireless sensor network for target detection, classification, and tracking," *Comput. Netw.*, vol. 46, no. 5, pp. 605–634, Dec. 2004. [Online]. Available: http://dx.doi.org/10.1016/j.comnet.2004.06.007

[6] P. Kulkarni, "Senseye: A multi-tier heterogeneous camera sensor network," Ph.D. dissertation, 2007, aAI3254905.

[7] V. Skvortsov, K. M. Lee, and S. E. Yang, "Inexpensive radar-based surveillance: Experimental study," in *International Conference Expo on Emerging Technologies for a Smarter World (CEWIT)*, Nov 2012.

[8] Z. Sun, P. Wang, M. C. Vuran, M. A. Al-Rodhaan, A. M. Al-Dhelaan, and I. F. Akyildiz, "Bordersense: Border patrol through advanced wireless sensor networks," *Ad Hoc Netw.*, vol. 9, no. 3.

[9] X. Zu, F. Guo, J. Huang, Q. Zhao, H. Liu, B. Li, and X. Yuan, "Design of an acoustic target intrusion detection system based on small-aperture microphone array," *Sensors*, vol. 17, no. 3, p. 514, 2017.

[10] M. J. Carlotto, "Detection and analysis of change in remotely sensed imagery with application to wide area surveillance," *IEEE Transactions on Image Processing*, vol. 6, no. 1, pp. 189–202, Jan 1997.

[11] J. C. R. Licklider and I. Pollack, "Effects of differentiation, integration, and infinite peak clipping upon the intelligibility of speech," *The Journal of the Acoustical Society of America*, vol. 20, no. 1, pp. 42–51, 1948.

[12] M. C. Bor, U. Roedig, T. Voigt, and J. M. Alonso, "Do lora low-power wide-area networks scale?" in *Proceedings of the 19th ACM International Conference on Modeling, Analysis and Simulation of Wireless and Mobile Systems*, 2016, pp. 59–67.